Journal of Orthopaedic Translation (2019) 17, 121—132

Available online at www.sciencedirect.com

ScienceDirect

journal homepage: http://ees.elsevier.com/jot

ORIGINAL ARTICLE

Surface degradation—enabled osseointegrative, angiogenic and antiinfective properties of magnesium-modified acrylic bone cement

Xiao Lin [a], Jun Ge [a], Donglei Wei [a], Chun Liu [a], Lili Tan [b], Huilin Yang [a,d], Ke Yang [b], Huan Zhou [c,d], Bin Li [a,d,***], Zong-Ping Luo [a,d,**], Lei Yang [a,d,*,1]

[a] *Orthopaedic Institute and Department of Orthopaedics, The First Affiliated Hospital, Soochow University, Suzhou, 215006, China*
[b] *Institute of Metal Research, Chinese Academy of Sciences, Shenyang, 110016, China*
[c] *School of Mechanical Engineering, Jiangsu University of Technology, Changzhou, 213001, China*
[d] *International Research Center for Translational Orthopaedics (IRCTO), Suzhou, 215006, China*

Received 2 February 2019; received in revised form 6 April 2019; accepted 29 April 2019
Available online 9 May 2019

KEYWORDS
Antiinfection;
Bone cement;
Kyphoplasty;
Magnesium;
Osseointegration

Abstract *Objective:* This work focuses on tackling the inadequate bone/implant interface strength of acrylic bone cements, which is a formidable problem diminishing their clinical performance, especially in percutaneous kyphoplasty surgery.
Methods: A new strategy of incorporating magnesium particles into clinically used poly(-methylmethacrylate) (PMMA) bone cement to prepare a surface-degradable bone cement (SdBC) is proposed and validated both *in vitro* and *in vivo*.
Results: This surface degradation characteristic enables osseointegrative, angiogenic and antiinfective properties. SdBC showed fast surface degradation and formed porous surfaces as designed, while the desirable high compressive strengths ($\geq$70 MPa) of the cement were preserved. Besides, the SdBC with proper Mg content promoted osteoblast adhesion, spreading, proliferation and endothelial cell angiogenesis capacity compared with PMMA. Also, SdBC demonstrated clear inhibitory effect on *Staphylococcus aureus* and *Escherichia coli*. *In vivo* evaluation on SdBC by the rat femur defect model showed that the bone/implant interface strength was significantly enhanced in SdBC (push-out force of 11.8 $\pm$ 1.5 N for SdBC vs

* Corresponding author. South Campus of Soochow University, 708 Renmin Road, Suzhou, Jiangsu 215006, China.
** Corresponding author. South Campus of Soochow University, 708 Renmin Road, Suzhou, Jiangsu 215006, China.
*** Corresponding author. South Campus of Soochow University, 708 Renmin Road, Suzhou, Jiangsu 215006, China.
E-mail addresses: binli@suda.edu.cn (B. Li), zongping_luo@yahoo.com (Z.-P. Luo), ylei@hebut.edu.cn (L. Yang).
[1] Present address: Center for Health Science and Engineering, School of Materials Science and Engineering, Hebei University of Technology, Tianjin 300310, China.

https://doi.org/10.1016/j.jot.2019.04.007

7.0 ± 2.3N for PMMA), suggesting significantly improved osseointegration and bone growth induced by the surface degradation of the cement. The injectability, setting times and compressive strengths of SdBC with proper content of Mg particles (2.8 wt% and 5.4 wt%) were comparable with those of the clinical acrylic bone cement, while the heat release during polymerization was reduced (maximum temperature 78 ± 1 °C for PMMA vs 73.3 ± 1.5 °C for SdBC).
Conclusions: This work validates a new concept of designing bioactive bone/implant interface in PMMA bone cement. And this surface-degradable bone cement possesses great potential for minimally invasive orthopaedic surgeries such as percutaneous kyphoplasty.
The translational potential of this article: This work reports PMMA/Mg surface-degradable acrylic bone cements that possess enhanced osseointegrative, angiogenic and antiinfective properties that are lacking in the clinically used acrylic bone cements. This new kind of bone cements could improve the treatment outcome of many orthopaedic surgeries such as percutaneous kyphoplasty and arthroplasty.

Introduction

Poly(methylmethacrylate) (PMMA)-based bone cements have been widely used in the current orthopaedic surgeries, including arthroplasty, treatments of femoral head osteonecrosis and spinal degenerative diseases. The fast polymerization and injectable capability of PMMA gives bone cement numerous advantages over preshaped implants, especially for the applications in the minimally invasive orthopaedic surgery (MIOS) such as percutaneous kyphoplasty (PKP) and vertebroplasty (PVP) [1,2]. Nevertheless, the need for improving PMMA rises because a large number of clinical cases indicate the risks of excessive heat released from acrylic monomer polymerization [3] and inadequate strength at the bone/cement interface, causing the instability of the interface or failure of the bone bonding to cement clump [4–7]. The inadequate interface strength was attributed to the lacks of osseointegrative and biodegrading ability of PMMA [8–10]. Modification of PMMA by incorporating bioactive or biodegradable additives has shown great potential to tackle these two problems simultaneously [9–13].

In addition, on the one hand, angiogenic capabilities become highly desirable for next-generation bone cement. Angiogenesis is critical for bone growth and regeneration, especially for diseases such as osteonecrosis. It is important for bone regeneration to build up a functional vascular network within the defect site, which can provide sufficient oxygen and nutrients to facilitate growth, differentiation and tissue functionality [14]. Also, the vascular invasion could reduce the risk of osteonecrosis around the bone substitutes. Angiogenic induction by bone cements itself is therefore a simple and efficacious strategy for bone regeneration and osteonecrosis prevention, which are important for enhancing strength at the bone/PMMA interface. On the other hand, bone cement–related infection has become a significant concern because of the increasing infection rate and the catastrophic consequences of infection [15–17]. The treatment for bone cement–related infection is however formidable, and the current resort of using antibiotics has created more hassles such as drug-resistance problems. Therefore, antiinfective bone cement without using antibiotics is highly desirable for orthopaedic surgery.

In this regard, the osseointegrative, angiogenic and antiinfective properties, as well as low heat release from polymerization, is desirable for bone cement, and relevant modifications of PMMA along this line become mainstream research directions in this area. Here, a strategy of designing surface-degradable bone cements (SdBCs) is reported, and the biodegradable Mg was selected as the degrading component of SdBC, which reveals translational potential to meet the needs of osseointegration, angiogenesis, and anti-infection at the same time. Bioactivity and biological properties of metallic Mg have recently been uncovered, and Mg alloys are designed as biodegradable materials primarily for orthopaedic applications [18–21]. This is largely due to elemental Mg being essential for bone development and metabolism and angiogenesis, which has also been reported in metallic Mg and its alloys [22–26]. Degradation of Mg and its alloys has also been reported to result in antibacterial effect due to the release of hydroxyl radicals and Mg^{2+} ions [27–29]. In addition, Mg and its alloy have tunable degradation rates *in vivo* [20,26]. Recent clinical studies have revealed the great translational potential of Mg alloys [30,31]. Thus, the present proof-of-concept study uses the aforementioned unique properties of Mg particles to modify clinically used PMMA bone cement, aiming at maintaining the feasibility of PMMA for MIOSs but simultaneously enhancing the bone/implant integration, angiogenesis and anti-infection performances of PMMA.

Materials and methods

Preparation of SdBC

OSTEOPAL V (Heraeus, Germany) PMMA bone cement and the commercially pure Mg particles (TangShan WeiHao Magnesium Powder Co., Ltd., Tangshan, China) with diameter of 100–150 μm were adopted for the preparation of SdBCs. In detail, 0.1, 0.2, 0.4 or 0.8 g of Mg particles were

mixed with 2.6 g PMMA powder. Then, 1 mL of methylmethacrylate (MMA) monomer was added in the mixed powder to form the SdBCs. The SdBCs were subsequently designated as 0.1-Mg, 0.2-Mg, 0.4-Mg and 0.8-Mg, the weight percentage of Mg particles being 2.7%, 5.3%, 10.2% and 18.4%, respectively. The PMMA was designated as 0-Mg for uniformity. Before the sample preparation, the Mg particles and OSTEOPAL V bone cement were kept at 23 ± 1°C for 2 h. The distributions of C, O, Mg and Zr elements in the cements were characterized by scanning electron microscopy (SEM, JSM-7100F, JEOL Ltd., Japan) and energy-dispersive spectrometry (OCTANE PRO, AMETEK Inc., USA).

In vitro degradation test

Cement cylinders with a diameter of 6 mm and height of 12 mm were immersed in Tris (tris(hydroxymethyl)aminomethane) buffer solution (pH = 7.4) with the immersion ratio of 1.25 cm^2/mL at 37 °C for up to 60 days. The solution was replaced every 2 days. The weight change [(final weigh − original weight)/original weight × 100%] of the samples and pH of solution were monitored. The inner microstructure and compressive properties of the bone cements before and after immersion were observed by SEM (Quanta 250, Thermo Fisher Scientific Inc., USA) and compressive tests on a mechanical tester (HY10000; Shanghai HengYi Precision Instrument Co., Ltd., Shanghai, China) at 20 mm/min, respectively. Before inner microstructure characterization, the samples were successively polished up to 2000 grit finish and then cleaned. The surface morphology of SdBCs after immersion was also characterized by SEM. The hydrophilicity of the cement was evaluated using a water contact angle metre (DSA 25S; Zeiss, Germany).

Characterization of handling properties

The maximum temperature during polymerization, doughing time and setting time of the cement was tested in reference to ISO5833: 2002 standard. The doughing time was indicated by failure of the material to stick to the surface of a surgically gloved probing finger. For maximum-temperature measurements, the cement pastes were mixed and cast in a cylindrical mold. The change in temperature during the setting reaction was measured under ambient conditions at 23 °C. The setting time was calculated according to the following formula: Setting time = $(T_{amb} + T_{max})/2$, where T_{amb} is the ambient temperature and T_{max} is the maximum temperature.

Injectability was defined as the weight percentage of cement capable of getting injected out of the syringe at the doughing time with a constant loading at 50 N. For direct comparison, the injectability of SdBC was normalized by PMMA.

Cytocompatibility test

MC3T3-E1 osteoblasts from the Type Culture Collection of Chinese Academy of Sciences (TCC, CAS, Shanghai, China) were selected for the cytocompatibility tests. α-Minimum essential medium (HyClone Laboratories Inc., USA) with 10 vol % foetal bovine serum (HyClone) and 1 vol % penicillin−streptomycin solution were used as the cell culture medium. All the cells were cultured in a humidified atmosphere of 5% CO_2 at 37 °C.

Cytocompatibility tests on material extracts

The samples (with same dimensions) were immersed in 75% ethanol for 30 min for sterilization and then rinsed by phosphate buffer saline (PBS) 3 times to remove the ethanol. After that, the samples were immersed in the cell culture media at an extraction ratio of 1.25 cm^2/mL at 37 °C for 1 day. The supernatant was withdrawn and filtrated through 0.22-μm membrane filter (Millex-GP; Millipore) for cell tests. The cell culture media incubating at 37 °C for 1 day was set as the control group.

Cells were cultured in material extracts at seeding density of 5000 cells/cm^2 for 1 and 3 days. Then, the cells were stained with LIVE/DEAD assay staining solution (Invitrogen™, Thermo Fisher Scientific Inc., USA) according to the manufacturer's instructions and then observed under a fluorescent microscope (EVOS, Thermo Fisher Scientific Inc., USA).

For cell counting kit-8 (CCK-8) assay, cells were cultured in 96-well plates in the presence of extracts for 1 and 3 days at a seeding density of 5000 cells/well. After prescribed times, the well was rinsed by 200 μL of PBS 2 times after removing the cell culture medium. Ten microlitres of CCK-8 (Dojindo Molecular Technologies, Inc) mixed in 100 μL of PBS was then added to each well and incubated at 37 °C for 2 h. Then, the solution was transferred out to a new 96-well plate for optical density (O.D.) measurements on a microplate reader (Power Wave X, BioTek Instruments, Inc., USA) at 450 nm. Cell viability = $O.D._{Extract}/O.D._{Media} \times 100\%$.

The pH value and Mg^{2+} concentration of extracts before and after 1 and 3 days of cell culture were measured using a pH metre and atomic absorption spectrometer (AA800, Perkin Elmer), respectively.

Cell adhesion test

Before experiments, the samples (with same dimensions) were polished, cleaned and sterilized as described in section Cytocompatibility tests on material extracts. Then, the osteoblasts were cultured on these samples for 1 and 3 days at a seeding density of 5000 cells/cm^2. After that, the samples were gently rinsed with PBS and then fixed with 2.5% glutaraldehyde for 4 h. Then, the samples were dehydrated with a series of ethanol solutions and finally dried using the critical point drying equipment (CPD300; Leica Instrument Co., Ltd., Germany) for SEM observation. The pH values of cell culture media after direct-contact cell culture for 1 and 3 days were measured.

Endothelial tube formation assay

Human umbilical vein endothelial cells (HUVECs) from the TCC, CAS were used for the tube formation test. Dulbecco's Modified Eagle Medium (DMEM, HyClone)-based culture media was used. Five hundred microlitres of Matrigel (Corning Co., Ltd., USA) was coated on each well of a 24-well plate. Then, the HUVECs were cultured on the Matrigel

in the presence of various extracts at a seeding density of 5000 cells/cm^2. The extracts were prepared using the DMEM-based cell culture media as described in section Cytocompatibility tests on material extracts. After 18 h, the tube formation was observed with an inverted phase contrast microscope (Axiocam 503; Carl Zeiss Co., Ltd., Germany). The images were analyzed using ImageJ (National Institutes of Health, USA) with the Angiogenesis Analyzer plugin to quantify the number of nodes, tubes and total length of network, per square millimetre.

Bacteria adhesion test

Staphylococcus aureus (*S. aureus* ATCC 25923) and *Escherichia coli* (*E. coli* ATCC 25922) were adopted in the test. The bacterial cells were propagated on an agar plate for 18—24 h at 37 °C to create colony-forming units (CFUs). One CFU from the plate was inoculated in Luria broth (LB) media to prepare bacterial suspensions, which were cultured in a shaking incubator at 190 rpm and 37 °C for 16—18 h, and then diluted with LB media for O.D. measurement at a wavelength of 670 nm to identify bacteria density in reference to the standard curve. Finally, the bacterial suspension was diluted with LB media to be 2.38×10^6 CFU/mL.

Samples (with same dimensions) were sterilized as descried in section Cytocompatibility tests on material extracts. Then, 1 mL of diluted bacterial suspension was added to the samples in the 24-well plate and incubated at 37 °C and 5% CO_2. After 24 h, the samples were fixed and dehydrated as described in section Cell adhesion test for SEM characterization. Four parallel samples were observed for each kind of bacteria.

In vivo study

The animal test plan and institutional ethical use protocols were approved by the ethics committee of the institutes the authors of the study are affiliated to. Six male Sprague—Dawley rats (weight, 400 ± 20 g) were used. All surgeries were performed under standard anaesthesia and disinfection procedures. Transcortical holes with a diameter of 2 mm were drilled at the same position of all femoral diaphysis under irrigation with saline after skin incision (1—2 cm long). 0-Mg and 0.2-Mg sample cylinders with a diameter of 1.9 mm and height of 8 mm were inserted into the holes of left and right femur, respectively. Finally, the incision was closed and animals were housed individually with normal access to food and water.

The rats were sacrificed at 2 months, and the retrieved tissue samples with implants were scanned using a micro—computed tomography (CT) scanner (Skyscan 1176; Bruker microCT) at an isometric resolution of 17 μm. The results were analyzed using the built-in analysis software. Owing to the similar contrast between bone and implant, the new bone formation was evaluated qualitatively through morphological analysis on three-dimensional (3D) reconstruction images.

Immediately after micro-CT analysis, half of specimens in each group were fixed in 4% paraformaldehyde for 2 days and then dehydrated and embedded in epoxy resin for SEM observation. The other half specimens were mounted on a test fixture for the push-out test at a displacement rate of 0.5 mm/min at a moist condition. The femur specimens after the push-out test were fixed in 4% paraformaldehyde for 2 days and then decalcified in ethylenediaminetetraacetic acid solution for histological analysis. Tissue sections (6-μm thick) were stained, respectively, by haematoxylin—eosin (H&E) and Masson trichrome staining method for transmitted light microscopy (AxioCam HRc; Zeiss) observation.

Statistical analysis

These measurements were run in at least three duplicates, and results were reported as the mean ± standard deviation calculated from repeated measurements. Statistical analysis of the cell proliferation results and endothelial tube formation results was conducted by one-way analysis of variance. All the pair-wise comparisons were performed by the *post hoc* test of Turkey. The two-tailed two-sample *t* test was used for the statistical analysis of push-out test results. When a p value was less than 0.05, significant differences were determined.

Results

Surface degradation behaviour of SdBCs

Addition of Mg particles did not affect the monomer polymerization of acrylic cement. After the cement was completely set, Mg particles appeared to evenly distribute in the PMMA matrix according to the SEM (Fig. 1A) and element distribution observation (Fig.S1), leading to homogeneous mechanical, degradation and biological properties of SdBCs. After immersion for 60 d, the interior of the SdBCs kept intact (Fig. 1A) because of no contacting with fluids, indicating that the Mg particles embedded inside the PMMA matrix would be a permanent second phase of the composite cement as expected, which is beneficial for preserving mechanical strength and tissue compatibility of the cement in the long-term implantation. In contrast, a great number of voids and pores were formed on the surface (Fig. 1B), of which the number increased with the increase of Mg content, confirming the surface-degradable property of the SdBCs. More importantly, the uniform distribution of Mg particles caused even surface degradation, indicating that the void size and density on the bone cement surface could be precisely controlled.

The surface degradation behaviour of SdBC was quantitatively confirmed by the weight loss of the samples (Fig. 1C). The percentage of weight loss was 0.3%, 2.3%, 2.6% and 5.7% for 0.1-Mg, 0.2-Mg, 0.4-Mg and 0.8-Mg, respectively, and all are much lower than the original weight percentage of Mg in each SdBC, indicating that only the Mg particles on the cement surface degraded. In addition, degradation of SdBCs slowed down gradually, probably because of the gradual loss of Mg on the cement surface and the protection formed by its degradation products [32,33]. The surface degradation behaviour of SdBCs also affected the chemical microenvironment adjacent to the cement. As a result of Mg degradation, the alkalinity was significantly altered as elevated pH values was observed in

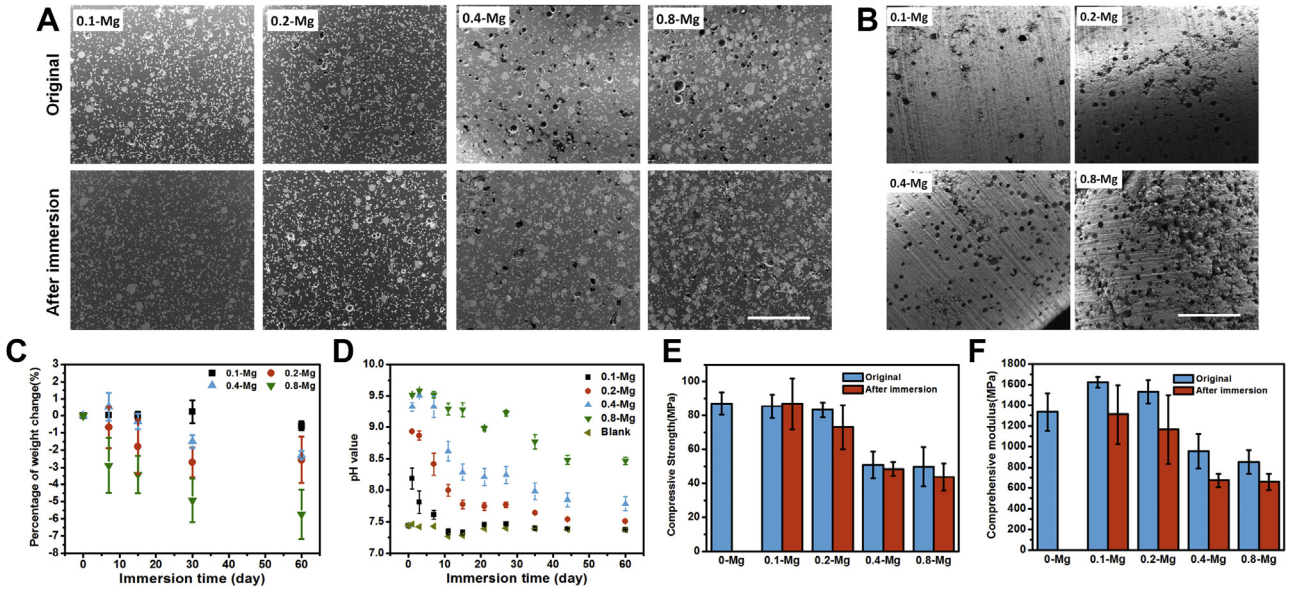

Figure 1 Surface degradation behavior of SdBCs. (A) SEM images of SdBCs before and after immersion in Tris solution for 60 d. The small white dots in the images are zirconium particles in the OSTEOPAL V bone cement as X-ray opaque agents. Scale bar, 1 mm. (B) Surface morphologies of SdBCs after immersion. Scale bar, 1 mm. (C) Percentage of weight change of SdBCs and (D) pH values of the immersion solution during immersion test. (E) Compressive strength and (F) compressive modulus of PMMA bone cement and SdBCs before and after immersion.
PMMA = poly(methylmethacrylate); SdBCs = surface-degradable bone cements; SEM = scanning electron microscopy.

the immersion fluid with SdBCs and correlated to the Mg content released (Fig. 1D).

Surface degradation of SdBCs however did not cause dramatic decrease in the compressive strength of cements (Fig. 1E). The decrease in the compressive strengths of SdBCs with the increasing initial content of Mg was probably due to the increased void density and the weakened Mg particle/PMMA interface strength [34]. The conservation of compressive strength during degradation is very important for load-bearing applications in orthopaedics and is a main advantage of the surface-degradable implant compared with the completely degradable cements such as calcium sulfates.

The greater compressive moduli of 0.1-Mg and 0.2-Mg compared to those of PMMA bone cement (Fig. 1F) should be attributed to the much higher modulus (~45 GPa) of metallic Mg than that of PMMA, agreeing with previous studies [35,36], while the lower compressive moduli of 0.4-Mg and 0.8-Mg compared to those of PMMA is probably due to the high density of voids in these SdBCs. The surface degradation of SdBCs decreased their compressive moduli and not compressive strength (Fig. 1F), which is beneficial for alleviating stress-shielding effect [37] or the secondary vertebra fracture when used for PKP [38].

Handling properties and hydrophilicity of SdBCs

The handling properties of the bone cement are crucial for minimally invasive surgical operation and the efficacy of PKP or percutaneous vertebroplasty (PVP). The doughing time and setting time of SdBCs were both lower than those of PMMA. When increasing the content of Mg, the doughing times of SdBCs decreased while the setting time first increased and then decreased (Fig. 2A). The injectability of SdBCs (Fig. 2B) increased first but then decreased when Mg content increased, and 0.4-Mg had the highest injectability, which should be attributed to the competing between rheological property of slurry and MMA polymerization reaction after Mg addition. The maximum temperature during the monomer polymerization of all the SdBCs (Fig. 2C) was lower than that of PMMA and decreased gradually when increasing the Mg content in different cements, which should be due to the decreased MMA fraction and enhanced thermal conductivity when increasing the content of Mg particles.

The hydrophilicity of bone cements is important for protein adsorption and bone tissue response *in vivo* [39,40], and higher surface hydrophilicity of bone cement is reportedly beneficial for tissue growth and bacteria inhibition [41]. Water contact angles on SdBCs were smaller than those on the PMMA (Fig. 2D), indicating higher surface hydrophilicity of SdBCs.

Cytocompatibility of SdBCs

As shown by the results of LIVE/DEAD assay after 1 d (Fig. 3A), osteoblasts in the extracts of PMMA, 0.1-Mg and 0.2-Mg grew better than those in the extracts of 0.4-Mg and 0.8-Mg. Nevertheless, osteoblasts in all the extracts exhibited obvious proliferation after 3 d, and few dead cells were observed. This proliferation result was confirmed by CCK-8 assay (Fig. 3B), which shows that the osteoblast proliferation at 1 d followed the trend 0.1-Mg > PMMA>0.2-Mg>0.4-Mg>0.8-Mg, while cells in all SdBC extracts proliferated better than those in PMMA extract and regular cell culture media after 3 d.

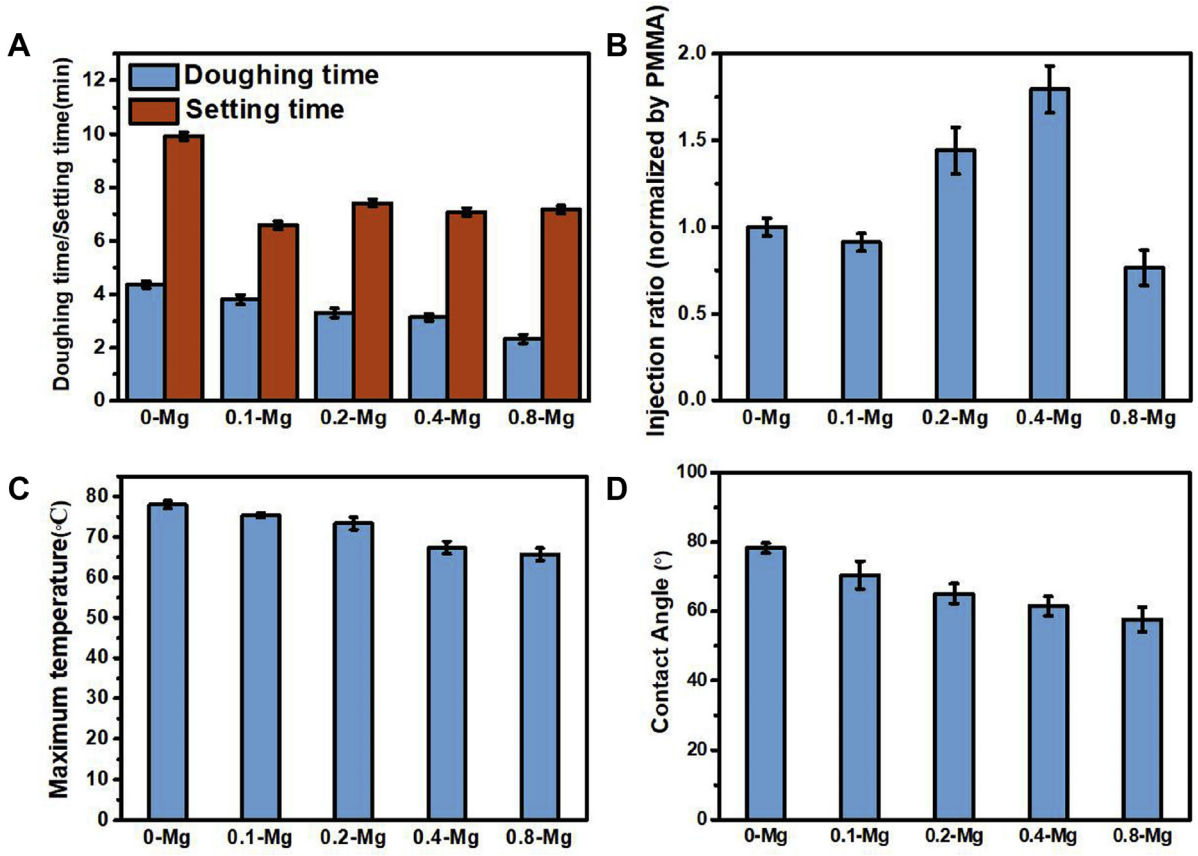

Figure 2 Handling properties and surface wettability of SdBCs. (A) Initial and final setting time and (B) injection ratio of PMMA and SdBCs. (C) Maximum temperature during polymerization of PMMA and SdBCs. (D) Water contact angle on PMMA and SdBCs. PMMA = poly(methylmethacrylate); SdBCs = surface-degradable bone cements.

Owing to surface degradation, the pH value and Mg^{2+} concentration of SdBC extracts significantly increased with the increase in Mg content of SdBCs (Fig. 3C and D). When used for cell culture, the pH values of all extracts decreased and the difference among the groups narrowed after 1 or 3 d. However, the Mg^{2+} concentration of each extract remained almost unchanged after cell culture. These results indicate that the decrease of cell viability from 0.1-Mg to 0.8-Mg at 1 d should be due to the acute toxic effects of high pH value rather than the high Mg^{2+} concentration of the extracts. In addition, the good cell viability of 0.4-Mg and 0.8-Mg groups at 3 d should be attributed to both the properly high Mg^{2+} concentration [42,43] and the decrease of pH (to a proper value that supports osteoblast proliferation [44]) of extracts in these groups.

The decreased cell viability with increasing Mg content at 1 d is probably due to the acute toxic effects of high pH values of the extracts, while the later increased cell proliferation at 3 d could be attributed to the gradually increased Mg^{2+} concentration and reduced pH value of the extracts.

SEM observation clearly showed that all osteoblasts on SdBCs exhibited better adhesion and spreading than the cells on PMMA at 1 d (Fig. 4A), which is consistent with the results reported in the previous work of poly(lactic-co-glycolic)/Mg alloy composite [45]. The worse adhesion and less spreading of osteoblasts on 0.4-Mg and 0.8-Mg compared to those on 0.1-Mg or 0.2-Mg are probably the adverse results of increased surface degradation of the cements. After culturing for 3 d, osteoblasts on all the samples showed better spreading than that after 1 d and the cell spreading on 0.1-Mg, 0.2-Mg and 0.4-Mg was similar and better than that on PMMA or 0.8-Mg. The pH increase of cell culture media during cell growth on samples (Fig. 4B) is milder than that without cell (Fig. 3C). Also, cells grew well on the Mg particles (Fig. 4C), demonstrating the high compatibility of degradable Mg particles.

In vitro angiogenic effect of SdBCs

In vitro angiogenesis test (Fig. 5) revealed that more nodes, tubes and networks were formed by HUVECs in 0.1-Mg and 0.2-Mg groups than by other Mg-containing samples. The 0.2-Mg group also exhibited better HUVEC network formation than 0-Mg and DMEM groups. The results indicate that the formation of HUVEC tubes was accelerated in the presence of proper concentration of Mg^{2+} and/or OH^{-} released from SdBCs.

Bacterial inhibitory effect of SdBCs

Surface degradation of SdBCs also resulted in the inhibitory effect of cements against *S. aureus* and *E. coli*. Fig. 6 shows that the density of *S. aureus* attached on SdBCs was

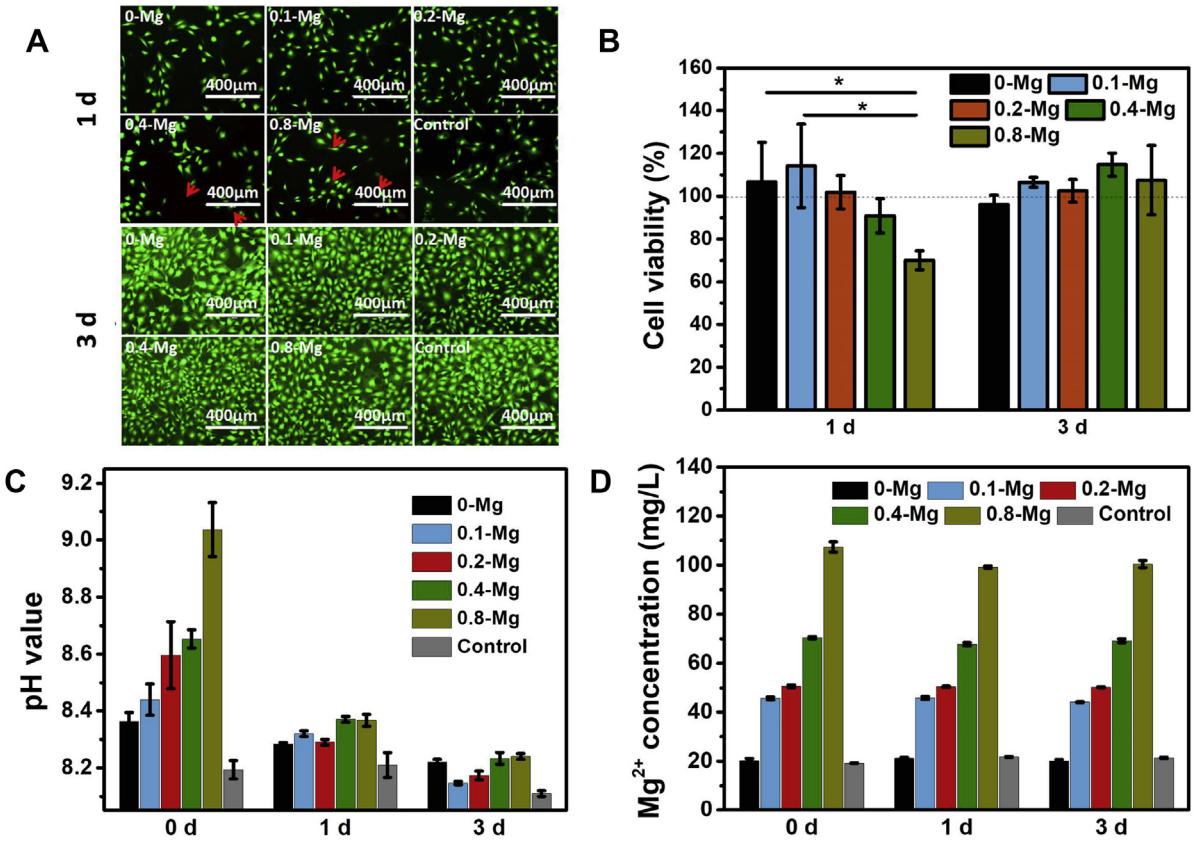

Figure 3 Cell viability in various material extracts. (A) Fluorescence micrographs of LIVE/DEAD—stained osteoblasts after cultured in different extracts for 1 and 3 d. The red arrows indicate dead cells. (B) Cell viabilities of different groups at 1 and 3 d. (C) pH value and (D) Mg^{2+} concentration of extracts before and after cell culture for 1 and 3 d.

significantly lowered than that on PMMA, and in fact, there were almost no bacterial aggregates on the SdBCs. The bacterial inhibitory effect of SdBCs against *S. aureus* was enhanced with the increasing Mg content in the cement, while interestingly, the inhibitory effect against *E. coli* was not significant and only 0.8-Mg showed obviously higher bacterial reduction than PMMA. The bacterial inhibitory effect of SdBCs should be due to the release of hydroxyl radicals and Mg^{2+} ions [27—29].

In vivo formation of bone/implant interface

The push-out test on the femurs after cement implantation for 2 m revealed that 0.2-Mg cement had significantly higher bone/implant interface strength than PMMA group (Fig. 7A), indicating more robust osseointegration *in vivo* between the surface-degraded 0.2-Mg cement and bone. More direct evidence by micro-CT indeed demonstrated considerably more trabecular bone formed around 0.2-Mg implant than that around PMMA in the bone marrow cavity (Fig. 7B), confirming the results of the push-out tests which implies higher osteogenic potential of 0.2-Mg cement than that of PMMA. More detailed inspection (Fig. 7C) showed the surface of PMMA remained smooth and intact after 2-m implantation, while a number of voids and pores formed on the surface of 0.2-Mg as a result of Mg degradation, which is also consistent with aforementioned surface degradation behaviour observed *in vitro*. Further examination of the bone/implant interface by back-scattered electron microscopy (Fig. 7D) shows smooth interface between bone and PMMA but zigzag interface between bone and 0.2-Mg cement. The observed zigzag pattern confirms the degradation of Mg particles on the surface of SdBC and subsequent bone ingrowth into the voids formed. Moreover, an interfacial layer was observed between the PMMA and cortical bone and it had similar image contrast to that of PMMA. H&E staining and Masson trichrome staining results (Fig. 7E) indicate this interfacial layer was a fibrous capsule that formed by connective tissue between the PMMA and ossification layer, agreeing with the results reported by others [13]. On contrary, direct bony contact was established between 0.2-Mg implant and bone, supported by the SEM and H&E and Masson trichrome staining results that a new compact bony layer was formed at the bone/implant interface.

Discussion

Previously, Mg particles or fibres have been added to biodegradable [34,36,45,46] or nondegradable and non-injectable [47] polymers for orthopaedic applications to enhance bioactivity. While in the present study, we proposed a surface-degradable and injectable bone cement, SdBC, through coupling biodegradable Mg particles with

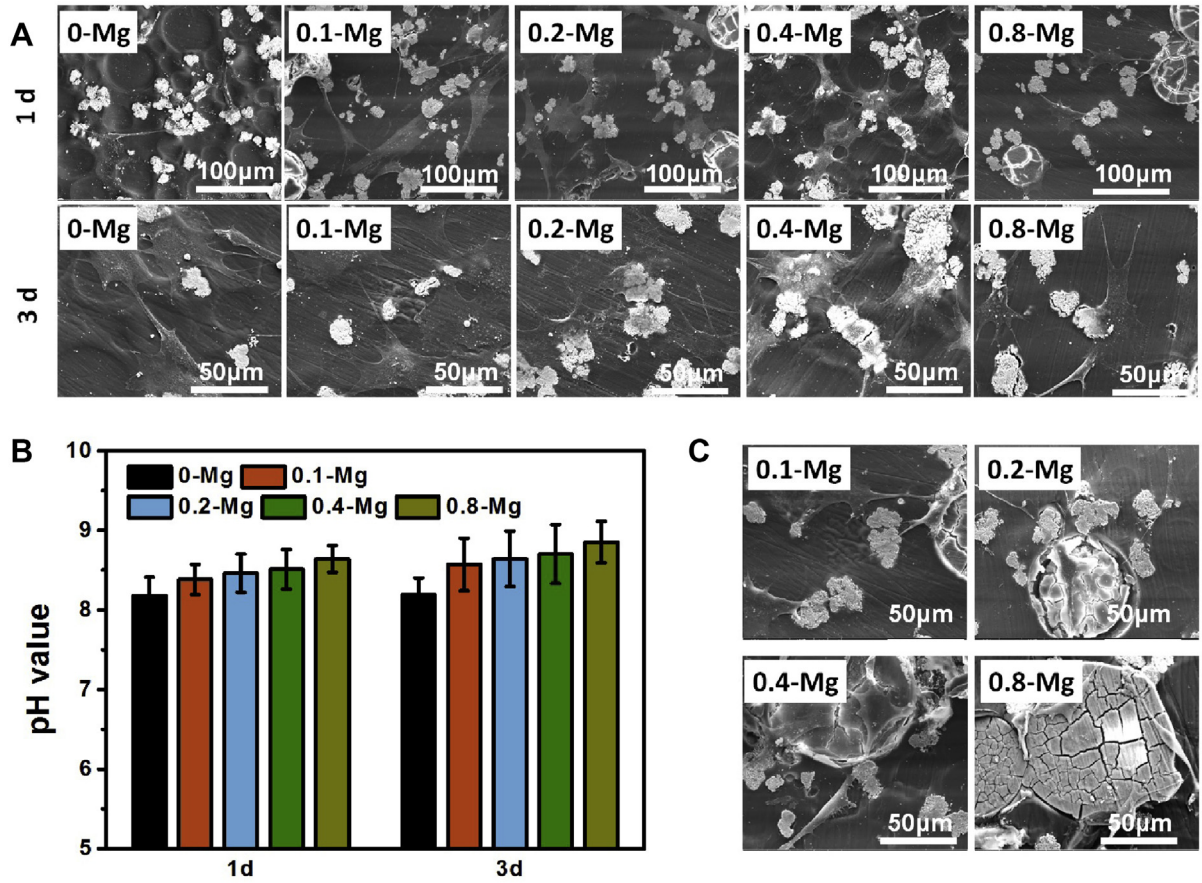

Figure 4 Cell spreading and viability on various samples. (A) Morphology of osteoblasts on the pristine PMMA bone cement and different SdBCs at 1 and 3 d. (B) pH of cell culture media after culturing for 1 and 3 d. (C) Morphology of osteoblasts on and around Mg particles in SdBCs at 1 d.
PMMA = poly(methylmethacrylate); SdBCs = surface-degradable bone cements.

nondegradable and injectable acrylic bone cement. SdBC owns several advantages compared with the totally degradable or noninjectable bone cements and is suitable for various orthopaedic surgeries, especially minimally invasive ones.

Unlike the totally degradable cements, surface-degradable characteristic of SdBCs benefits the maintenance of excellent mechanical strength (Fig. 2D) *in vivo*, which is critical for load-bearing applications. The compressive modulus of SdBCs could decrease by about 20% after degradation (Fig. 1F), which could alleviate stress-shielding effects [37] of stiff PMMA or the secondary vertebra fracture usually caused by acrylic cements in PKP [38].

Degradation of Mg particles at the surface of SdBCs releases hydroxyl, Mg^{2+} and H_2 gas and alters the surface morphology and chemical composition of SdBCs. These factors will synergistically affect the biological response to the cement, and this mechanism is lacking in the nondegradable cements. First, osteoblasts adhered and spread better on the 0.1-Mg and 0.2-Mg samples than on the PMMA (Fig. 3A), which should be attributed to the proper Mg^{2+} concentration around these SdBCs and the CaP and MgP deposition on the SdBC surface, both facilitating osteoblast growth [48]. Osteoblasts appeared to be more sensitive to hydroxyl ions rather than Mg^{2+} ions release from SdBCs (Fig. 4), which has been reported before [49,50]. Meanwhile, the released hydroxyl could be neutralized dynamically during osteoblast growth directly on SdBCs. It could be expected that after *in vivo* implantation, the hydroxyl released from Mg would be neutralized simultaneously by tissue metabolism and circulation of body fluids as seen *in vitro* (Fig. 3B). Second, 0.2-Mg showed enhanced angiogenic and osteogenic capacities, which are lacking in PMMA and are probably the result of Mg^{2+} release at proper concentration [25]. Third, the inhibitory effect of the SdBCs against *S. aureus* and *E. coli* was much better than that of PMMA, which could prevent the implant-related infection [51]. However, the bacterial inhibitory effect is not as significant as that of bulk Mg implant [27—29], which should be owed to the inadequate ion release from SdBCs. This study also reveals that increasing the Mg content of SdBCs was beneficial for antibacterial capability but could deteriorate other properties of SdBC. Preparing SdBCs using strongly antibacterial Mg alloy [52—54] particles is a promising way to further enhance their antibacterial properties. Fourth, surface degradation strategy leads to voids and pores that formed on the surface of SdBCs after degradation (Fig. 2B) for subsequent tissue ingrowth, forming a bone/implant

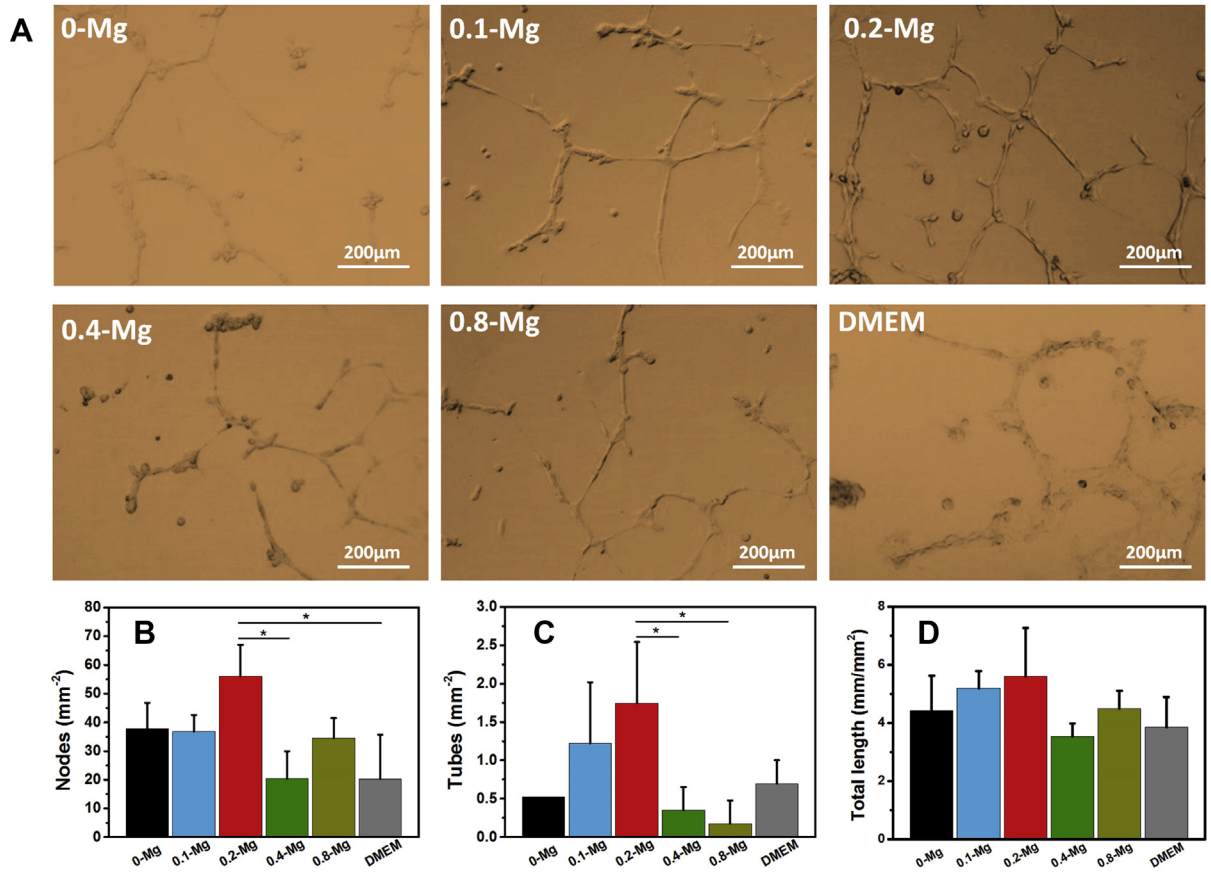

Figure 5 *In vitro* angiogenesis of HUVECs cultured on the Matrigel basement membrane matrix in the presence of different extracts at 18 h. (A) Typical images in different groups. (B) The number of tubes, (C) number of nodes and (D) total length of network, per square millimetre.
HUVECs = human umbilical vein endothelial cells.

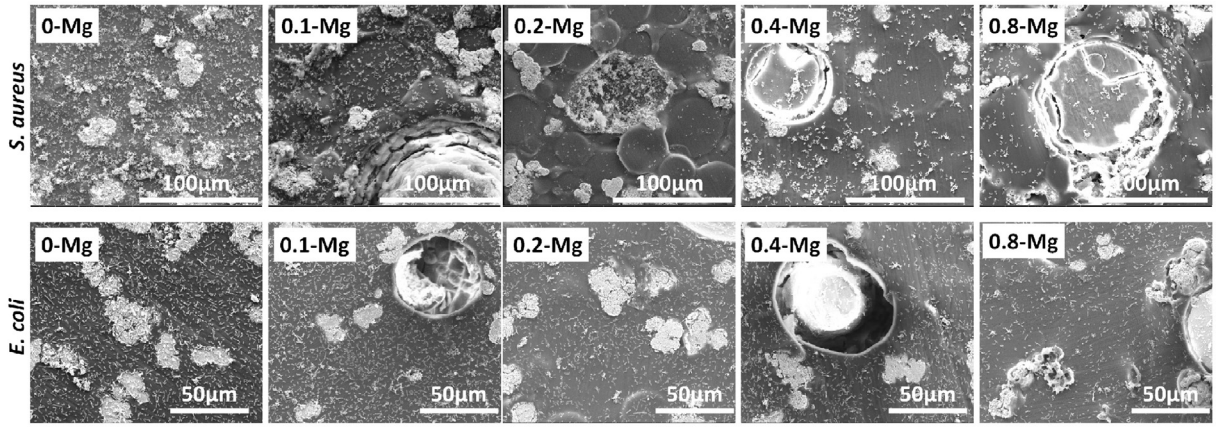

Figure 6 *S. aureus* and *E. coli* adhesion on various samples at 24 h observed by SEM.
SEM = scanning electron microscopy.

physical interlocking eventually. The high interface strength is important for long-term stability of the bone/implant interface. The bone/cement interface strength of 0.2-Mg SdBC measured by push-out force was significantly higher than that of PMMA, suggesting a strong physical interlocking mechanism between bone and SdBC, as well as enhanced bone formation and osseointegration. The bone/cement interface strength could increase with prolonging of implantation time according to previous works [55,56].

The SdBCs maintained the injectable characteristic of PMMA bone cement for MIOSs. The relatively short doughing time of SdBCs enables surgeons to start injection procedure sooner. Also, sufficient working time (indicated by the

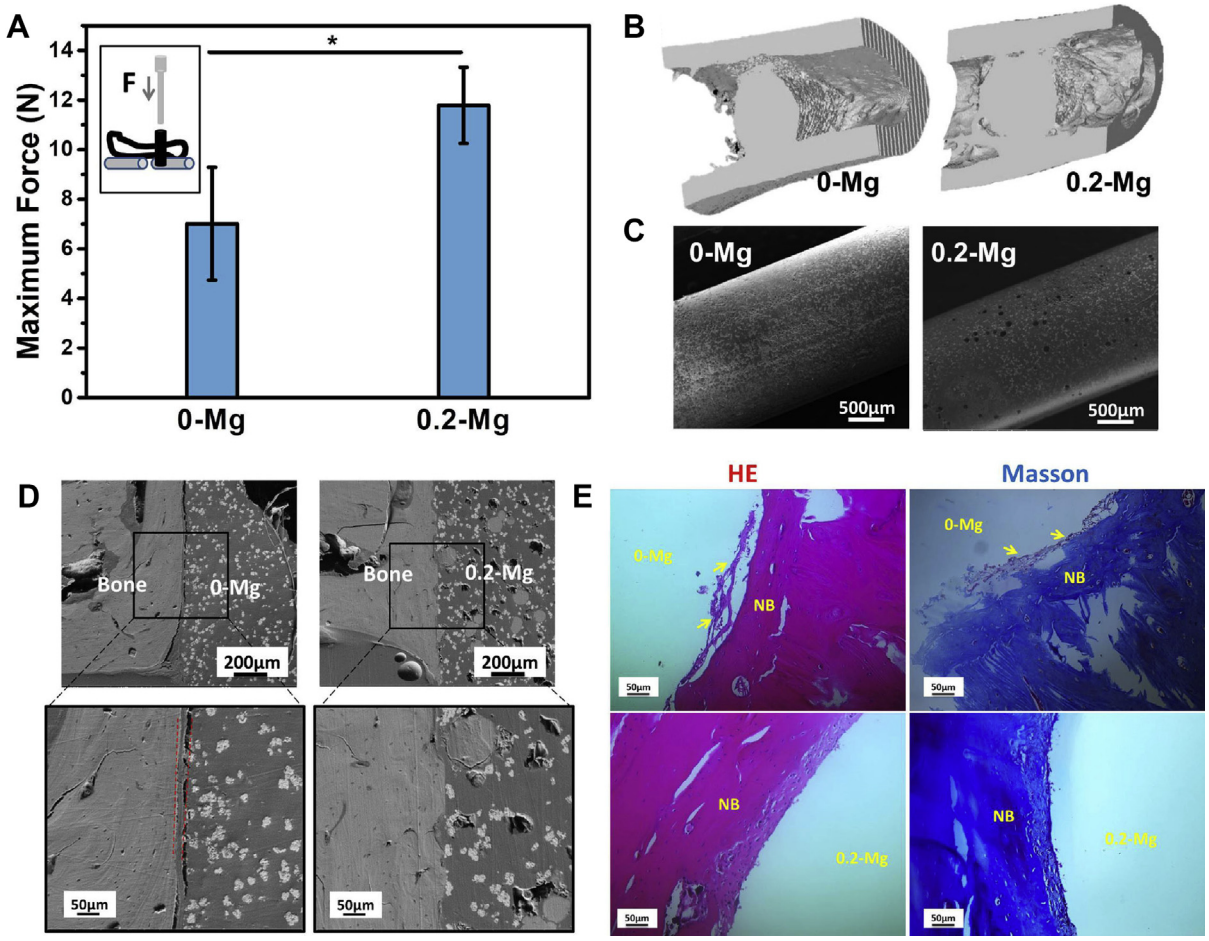

Figure 7 *In vivo* bone response evaluations. (A)Maximum force obtained from biomechanical push-out test. The inset shows setup for push-out test. *, $p < 0.05$. (B) 3D micro-CT images of the femur around implant obtained from the longitudinal viewpoint at 2 m of implantation. (C) Surface morphology of samples and (D) bone/implant interface morphology at 2 m of implantation, observed by SEM. (E) H&E-stained and Masson trichrome—stained slices of periimplant bone tissue at 2 m. NB = new bone. "0-Mg" and "0.2-Mg" indicate the initial implant site. Arrows point the fibrous capsule.
CT = computed tomography; H&E = haematoxylin—eosin; SEM = scanning electron microscopy.

setting time) is essential for appropriate handling and deployment of cements, and typically, the surgeon needs 6—8 min to mix and inject the cement in PVP [57]. SdBCs had acceptable setting times for minimally invasive surgery, and typical setting time was between 6.6 and 7.4 min. In addition, the injectability of 0.1-Mg, 0.2-Mg and 0.4-Mg would meet the requirement for clinical use and the improvement of injectability by adding 5.4 wt% to 10.3 wt% of Mg particles, agreeing with previous studies [12,58]. The reduction of potentially harmful high temperature during PMMA polymerization by adding Mg particles is another important advantage of SdBCs [3].

Although the present study exhibits many advantages of SdBC, it should be optimized to meet the clinical requirements of MIOS, including the handling, materials and biological properties, especially the angiogenic and antibacterial capabilities. The Mg particle concentration greatly influences the handling and material properties of SdBC, and another factor could be the size of Mg particles. Optimal biological properties of SdBCs could be realized by adding proper content of Mg with proper composition. Especially, Mg alloys with elements that reportedly have osteogenic, angiogenic and antibacterial properties [41,52—54] should be adopted. Degradation rate [20] and size of Mg particles should be optimized to promote bone ingrowth on SdBCs [59]. Future directions should be focused on the optimization of the composite bone cements by adjusting the content, size and composition of Mg particles. Long-term *in vivo* study was also necessary to evaluate the long-term bone/implant interface, local bone response and systematic biosafety.

Conclusions

The present study demonstrated a novel and effective strategy of developing surface-degradable PMMA/Mg bone cements that possess environmentally responsive surface, leading to a porous surface for bone ingrowth while preserving the high compressive strength of acrylic cement. The surface-degradation induced by Mg particles creates a proper ionic vicinity around the bone cement, which promotes osteoblasts activity and tube formation of HUVECs and inhibits bacterial adhesion on the cement surface.

SdBC also maintains the similar handling and setting properties as the clinically used acrylic cements. *In vivo* evaluation suggested that the interfical strength at the bone/SdBC interface was significantly higher than that at the bone/PMMA interface because of enhanced bone ingrowth and subsequent osseointegration. This work validates a new concept of designing bioactive bone/implant interface with desirable properties. This surface degradation strategy assisted by Mg particles therefore has great potential to revolutionize the currently used acrylic cements for greatly improving the efficacy and outcomes of minimally invasive surgeries.

Acknowledgements

This work was supported by the National Natural Science Foundation of China [81501858, 81622032 and 51672184], Jiangsu Innovation and Entrepreneurship Program, National Basic Research Program of China [973 Program, 2014CB748600] and the Priority Academic Program Development of Jiangsu High Education Institutions (PAPD).

Appendix A. Supplementary data

Supplementary data to this article can be found online at https://doi.org/10.1016/j.jot.2019.04.007.

Conflict of interests

The authors have no conflicts of interest relevant to this article.

References

[1] Ali U, Karim KJ, Buang NA. A review of the properties and applications of poly (methyl methacrylate) (PMMA). Polym Rev 2015;55(4):1—28.
[2] He Z, Zhai Q, Hu M, Cao C, Wang J, Yang H, et al. Bone cements for percutaneous vertebroplasty and balloon kyphoplasty: current status and future developments. J Orthop Translat 2015;3(1):1—11.
[3] Castaldini A, Cavallini A. Setting properties of bone cement with added synthetic hydroxyapatite. Biomaterials 1985;6(1):55—60.
[4] Sundfeldt M, Carlsson LV, Johansson CB, Thomsen P, Gretzer C. Aseptic loosening, not only a question of wear: a review of different theories. Acta Orthop 2006;77(2):177—97.
[5] Lewis G. Properties of acrylic bone cement: State of the art review. J Biomed Mater Res B 1997;38(2):155—82.
[6] Ries MD, Young E, Al-Marashi L, Goldstein P, Hetherington A, Petrie T, et al. In vivo behavior of acrylic bone cement in total hip arthroplasty. Biomaterials 2006;27(2):256—61.
[7] Goodheart JR, Miller MA, Mann KA. In vivo loss of cement-bone interlock reduces fixation strength in total knee arthroplasties. J Orthop Res 2014;32(8):1052—60.
[8] Heo SJ, Park SA, Shin HJ, Lee YJ, Yoon TR, Seo HY, et al. Evaluation of bonding stress for the newly suggested bone cement: comparison with currently used PMMA through animal studies. Key Eng Mater 2007;342-343:373—6.
[9] Wolf-Brandstetter C, Roessler S, Storch S, Hempel U, Gbureck U, Nies B, et al. Physicochemical and cell biological characterization of PMMA bone cements modified with additives to increase bioactivity. J Biomed Mater Res B 2013;101B(4):599—609.
[10] Khandaker M, Li Y, Morris T. Micro and nano MgO particles for the improvement of fracture toughness of bone-cement interfaces. J Biomech 2013;46(5):1035—9.
[11] Tan H, Guo S, Yang S, Xu X, Tang T. Physical characterization and osteogenic activity of the quaternized chitosan-loaded PMMA bone cement. Acta Biomater 2012;8(6):2166—74.
[12] Kim SB, Kim TJ, Yoon TL, Su AP, Cho IH, Kim EJ, et al. The characteristics of a hydroxyapatite—chitosan—PMMA bone cement. Biomaterials 2004;25(26):5715—23.
[13] Cimatti B, Santos MA, Brassesco MS, Okano LT, Barboza WM, Nogueirabarbosa MH, et al. Safety, osseointegration, and bone ingrowth analysis of PMMA-based porous cement on animal metaphyseal bone defect model. J Biomed Mater Res B 2017;106(10):649—58.
[14] Brey EM, King TW, Johnston C, Mcintire LV, Reece GP, Patrick Jr CW. A technique for quantitative three-dimensional analysis of microvascular structure. Microvasc Res 2002;63(3):279—94.
[15] Hendriks JG, van Horn JR, van der Mei HC, Busscher HJ. Backgrounds of antibiotic-loaded bone cement and prosthesis-related infection. Biomaterials 2004;25(3):545—56.
[16] Ridgeway S, Wilson J, Charlet A, Kafatos G, Pearson A, Coello R. Infection of the surgical site after arthroplasty of the hip. J Bone Joint Surg Br 2005;87(6):844—50.
[17] Ying Y, Ao H, Wang Y, Lin W, Yang S, Zhang S, et al. Cytocompatibility with osteogenic cells and enhanced in vivo antiinfection potential of quaternized chitosan-loaded titania nanotubes. Bone Res 2016;4(3):140—53.
[18] Staiger MP, Pietak AM, Huadmai J, Dias G. Magnesium and its alloys as orthopedic biomaterials: a review. Biomaterials 2006;27(9):1728—34.
[19] Witte F. The history of biodegradable magnesium implants: a review. Acta Biomater 2010;6(5):1680—92.
[20] Zheng Y, Gu X, Witte F. Biodegradable metals. Mater Sci Eng R 2014;77(2):1—34.
[21] Lin X, Tan L, Wang Q, Zhang G, Zhang B, Yang L. In vivo degradation and tissue compatibility of ZK60 magnesium alloy with micro-arc oxidation coating in a transcortical model. Mater Sci Eng C-Mater 2013;33(7):3881—8.
[22] Witte F, Kaese V, Haferkamp H, Switzer E, Meyer-Lindenberg A, Wirth CJ, et al. In vivo corrosion of four magnesium alloys and the associated bone response. Biomaterials 2005;26(17):3557—63.
[23] Castellani C, Lindtner RA, Hausbrandt P, Tschegg E, Stanzl-Tschegg SE, Zanoni G, et al. Bone-implant interface strength and osseointegration: biodegradable magnesium alloy versus standard titanium control. Acta Biomater 2005;7(1):432—40.
[24] Zhang Y, Xu J, Ruan Y, Yu MK, O'Laughlin M, Wise H, et al. Implant-derived magnesium induces local neuronal production of CGRP to improve bone-fracture healing in rats. Nat Med 2016;22(10):1160—9.
[25] Bose S, Fielding G, Tarafder S, Bandyopadhyay A. Understanding of dopant-induced osteogenesis and angiogenesis in calcium phosphate ceramics, Trends. Biotechnology 2013;31(10):594—605.
[26] Wang J, Wu Y, Li H, Liu Y, Bai X, Chau W, et al. Magnesium alloy based interference screw developed for ACL reconstruction attenuates peri-tunnel bone loss in rabbits. Biomaterials 2017;157:86—97.
[27] Robinson DA, Griffith RW, Dan S, Evans RB, Conzemius MG. In vitro antibacterial properties of magnesium metal against Escherichia coli , Pseudomonas aeruginosa and Staphylococcus aureus. Acta Biomater 2010;6(5):1869—77.
[28] Li Y, Liu G, Zhai Z, Liu L, Li H, Yang K, et al. Antibacterial properties of magnesium in vitro and in an in vivo model of implant-associated methicillin-resistant Staphylococcus

aureus infection. Antimicrob Agents Chemother 2014;58(12):7586—91.
[29] Feng H, Wang G, Jin W, Zhang X, Huang Y, Gao A, et al. Systematic study of inherent anti-bacterial properties of magnesium-based biomaterials. Acs Appl Mater Inter 2016;8(15):9662—73.
[30] Zhao D, Huang S, Lu F, Wang B, Yang L, Qin L, et al. Vascularized bone grafting fixed by biodegradable magnesium screw for treating osteonecrosis of the femoral head. Biomaterials 2016;81(1):84—92.
[31] Lee J, Han H, Han K, Park J, Jeon H, Ok M, et al. Long-term clinical study and multiscale analysis of in vivo biodegradation mechanism of Mg alloy. Proc Natl Acad Sci USA 2016;113(3):716—21.
[32] Lin X, Tan L, Zhang Q, Yang K, Hu Z, Qiu J, et al. The in vitro degradation process and biocompatibility of a ZK60 magnesium alloy with a forsterite-containing micro-arc oxidation coating. Acta Biomater 2013;9(10):8631—42.
[33] Lin X, Yang X, Tan L, Li M, Wang X, Zhang Y, et al. In vitro degradation and biocompatibility of a strontium-containing micro-arc oxidation coating on the biodegradable ZK60 magnesium alloy. Appl Surf Sci 2014;288(2):718—26.
[34] Wan P, Yuan C, Tan L, Li Q, Yang K. Fabrication and evaluation of bioresorbable PLLA/magnesium and PLLA/magnesium fluoride hybrid composites for orthopedic implants. Compos Sci Technol 2014;98:36—43.
[35] Cifuentes SC, Frutos E, González-Carrasco JL, Muñoz M, Multigner M, Chao J, et al. Novel PLLA/magnesium composite for orthopedic applications: a proof of concept. Mater Lett 2012;74(5):239—42.
[36] Wong HM, Wu S, Chu PK, Cheng SH, Luk KD, Cheung KM, et al. Low-modulus Mg/PCL hybrid bone substitute for osteoporotic fracture fixation. Biomaterials 2013;34(29):7016—32.
[37] Nagels J, Stokdijk M, Rozing PM. Stress shielding and bone resorption in shoulder arthroplasty. J Shoulder Elb Surg 2003;12(1):35—9.
[38] Kolb JP, Kueny RA, Püschel K, Boger A, Rueger JM, Morlock MM, et al. Does the cement stiffness affect fatigue fracture strength of vertebrae after cement augmentation in osteoporotic patients? Eur Spine J 2013;22(7):1650—6.
[39] Wei J, Igarashi T, Okumori N, Igarashi T, Maetani T, Liu B, et al. Influence of surface wettability on competitive protein adsorption and initial attachment of osteoblasts. Biomed Mater 2009;4(4):045002.
[40] Eriksson C, Nygren H, Ohlson K. Implantation of hydrophilic and hydrophobic titanium discs in rat tibia: Cellular reactions on the surfaces during the first 3 weeks in bone. Biomaterials 2004;25(19):4759—66.
[41] Lin X, Yang S, Lai K, Yang H, Webster TJ, Yang L. Orthopedic implant biomaterials with both osteogenic and anti-infection capacities and associated in vivo evaluation methods. Nanomedicine: NBM (NMR Biomed) 2016;13(1):123—42.
[42] He L, Zhang X, Liu B, Tian Y, Ma W. Effect of magnesium ion on human osteoblast activity. Braz J Med Biol Res 2016;49(7):e5257.
[43] Abed E, Moreau R. Importance of melastatin-like transient receptor potential 7 and cations (magnesium, calcium) in human osteoblast-like cell proliferation. Cell Prolif 2007;40(6):849—65.
[44] Pan H, Shen Y, Wen C, Peng S, Lu WW. Role of pH-The essential step for osteoporotic bone regeneration. Bone 2010;47(S3):S444.
[45] Cheng YH, Zheng TF. In vitro study on biodegradable AZ31 magnesium alloy fibers reinforced PLGA composite. J Mater Sci Technol 2013;29(6):545—50.
[46] Brown A, Zaky S, Jr RH, Sfeir C. Porous magnesium/PLGA composite scaffolds for enhanced bone regeneration following tooth extraction. Acta Biomater 2015;11:543—53.
[47] Jung HD, Hui SP, Kang MH, Lee SM, Kim HE, Estrin Y, et al. Polyetheretherketone/magnesium composite selectively coated with hydroxyapatite for enhanced in vitro biocorrosion resistance and biocompatibility. Mater Lett 2014;116(2):20—2.
[48] Xin Y, Chu PK. In vitro studies of biomedical magnesium alloys in a simulated physiological environment: a review. Acta Biomater 2011;7(4):1452—9.
[49] Seuss F, Seuss S, Turhan MC, Fabry B, Virtanen S. Corrosion of Mg alloy AZ91D in the presence of living cells. J Biomed Mater Res B 2011;99B(2):276—81.
[50] Wong HM, Yeung KW, Lam KO, Tam V, Chu PK, Luk KD, et al. A biodegradable polymer-based coating to control the performance of magnesium alloy orthopaedic implants. Biomaterials 2010;31(8):2084—96.
[51] An YH, Friedman RJ. Concise review of mechanisms of bacterial adhesion to biomaterial surfaces. J Biomed Mater Res B 2015;43(3):338—48.
[52] Tie D, Feyerabend F, Müller WD, Schade R, Liefeith K, Kainer KU, et al. Antibacterial biodegradable Mg-Ag alloys. Eur Cells Mater 2013;25:284—98.
[53] Li Y, Liu L, Wan P, Zhai Z, Mao Z, Ouyang Z, et al. Biodegradable Mg-Cu alloy implants with antibacterial activity for the treatment of osteomyelitis: in vitro and in vivo evaluations. Biomaterials 2016;106:250—63.
[54] Liu C, Fu X, Pan H, Wan P, Wang L, Tan L, et al. Biodegradable Mg-Cu alloys with enhanced osteogenesis, angiogenesis, and long-lasting antibacterial effects. Sci Rep-UK 2016;6:27374.
[55] Lye KW, Tideman H, Wolke JC, Merkx MA, Chin FK, Jansen JA. Biocompatibility and bone formation with porous modified PMMA in normal and irradiated mandibular tissue. Clin Oral Implant Res 2013;24(A100):100—9.
[56] Dai KR, Liu YK, Park JB, Clark CR, Nishiyama K, Zheng ZK. Bone-particle-impregnated bone cement: an in vivo weight-bearing study. J Biomed Mater Res 1991;25(2):141—56.
[57] Hide IG, Gangi A. Percutaneous vertebroplasty: history, technique and current perspectives. Clin Radiol 2004;59(6):461—7.
[58] Vallo CI, Montemartini PE, Fanovich MA, Porto López JM, Cuadrado TR. Polymethylmethacrylate-based bone cement modified with hydroxyapatite. J Biomed Mater Res B 2015;48(2):150—8.
[59] Murphy CM, Haugh MG, O'Brien FJ. The effect of mean pore size on cell attachment, proliferation and migration in collagen—glycosaminoglycan scaffolds for bone tissue engineering. Biomaterials 2010;31(3):461—6.